Arc-seamount collision: driver for vertical-axis rotations in Azuero, Panama

LUIS A. RODRIGUEZ-PARRA[1], CAMILO GAITÁN[1], CAMILO MONTES[1], GERMÁN BAYONA[2] AND AUGUSTO RAPALINI[3]

1 Departamento de Geociencias, Universidad de los Andes, Bogotá, Colombia (la.rodriguez1876@uniandes.edu.co)

2 Corporación Geológica Ares, Bogotá, Colombia

3 Instituto de Geociencias Básicas, Aplicadas y Ambientales de Buenos Aires, Universidad de Buenos Aires - CONICET, Buenos Aires, Argentina

Received: July 16, 2016; Revised: Novemebr 21, 2016; Accepted: November 25, 2016

ABSTRACT

We present new paleomagnetic data of 25 sites (240 specimens) along the southwestern part of the Azuero Peninsula, Panama. The data show two paleomagnetic domains in the peninsula: a northern domain featuring uniformly large vertical-axis clockwise rotation values of 73.4 ± 12° across to Azuero Soná Fault Zone with a single mean direction with declination of 81.2° and inclination of –3.2° (95% confidence of 11.7° and precision parameter of 18.09), and a scattered paleomagnetic domain to the south. These contrasting domains could be attributed to the collision of far-travelled/allochthonous seamounts that approached the Panama arc as subduction of the Farallon plate brought them to the margin. As consequence of this collision the far-travelled seamounts were fragmented and scattered along the margin while the Panama arc rotated into the colliding seamounts. These new paleomagnetic data suggest that the Campanian-Eocene arc segment in the Azuero Peninsula was originally oriented NE-SW, implying an original curvature for this part of the arc.

Keywords: paleomagnetism, collision-induced rotation, paleogeography, Panamanian Arc

1. INTRODUCTION

Tectonic block rotations in forearcs of active convergent plate margins are events that can be recorded using global positioning system (GPS) (e.g., Papua New Guinea). *Wallace et al. (2005)* suggest that forearc rotations are the product of a buoyant indentor entering a subduction zone, for example the accretion of seamounts. Previous lithologic observations and geochemical studies of the Azuero Peninsula, Panama (e.g., *Buchs et al., 2011a*) suggest the accretion of seamounts along the trailing edge of the Caribbean plate. The Azuero Peninsula is an excellent area to study the relationship between seamount collision and magmatic arcs because it exposes a deformed, fragmented forearc where the collisional processes can be directly observed and studied.

Buchs et al. (2011b) and *Mann and Corrigan (1990)* suggest that the Azuero Soná Fault Zone (ASFZ) separates autochthonous from far-travelled/allochthonous terrains. The geology and tectonic evolution of each block is different, including age, geochemistry, stratigraphy, granting this distinction (*Buchs et al., 2011a*). However, the effects of the processes that brought these seamounts to the subduction margin of the Panama arc have not been investigated. Collision and accretion must have modified the margin, and probably would have also affected magmatic processes in the arc (*McCabe, 1984*; *Vogt et al., 1976*; *Wallace et al., 2005*).

We present new paleomagnetic results from sites sampled during 2014 and 2015 in the southwestern part of the Azuero Peninsula, distributed in different blocks located both in the north and south of ASFZ. We took advantage of layered basalt flows and interbedded fine-grained sedimentary rocks as markers of the paleo-horizontal references, which then we used as a bedding correction of paleomagnetic data. Our data reveals consistent, large vertical-axis rotations in tectonic blocks around the ASFZ, but scattered in the seamount domain to the south. These new data document the process of seamount collision, accretion and arc rotation in the trailing edge of the Caribbean plate.

2. REGIONAL GEOLOGY

2.1. Panamanian Isthmus

The Isthmus of Panama is located at the southwestern trailing edge of the Caribbean plate (*Pindell and Kennan, 2009*), in the junction between Nazca, Cocos, Caribbean and South American plates (*Molnar and Sykes, 1969*; Fig. 1). It is composed by Cenozoic and Mesozoic magmatic products (*Buchs et al., 2010*, *2011b*; *Whattam et al., 2012*) and several sedimentary overlapping sequences (*Coates and Obando, 1996*; *Kolarsky et al., 1995*). The magmatic products are the result of three main processes: an oceanic plateau extrusion (the Caribbean Large Igneous Province, CLIP), an Upper Cretaceous and younger arc system in southern Costa Rica and western Panama (*Drummond et al., 1995*; *Kesler, 1978*; *Whattam et al., 2012*), and finally seamount accretion (*Buchs et al., 2010*, *2011a*; *Lissinna, 2005*; *Wegner et al., 2011*). Additionaly, there are periods without magmatism and even sedimentation processes related with deformational events in the Isthmus (*Mann and Corrigan, 1990*; *Montes et al., 2012*; *Silver et al., 1990*).

The Panama Ishmus is bound to the north by a submarine deformed belt and its associated earthquake and shorteninng processes (*Pennigton, 1981*; *Silver et al., 1995*). To the east, the Uramita Fault (*Duque-Caro, 1990*) is located between a volcanic basement and the Chuqunaque basin, which has been interpreted as an extension of the Atrato basin (*Montes et al., 2012*). The south boundary is constituted by left-lateral and normal subduction west of Azuero Peninsula (*Montes et al., 2012*), and an accretionary complex through Costa Rica and Western Panama. Finally, the western boundary is a broad zone of well distributed left-lateral shear in central Costa Rica (*Camacho et al., 2010*; *Fan et al., 1991*).

Paleomagnetic studies have helped to reconstruct a model of the deformational events of the Isthmus. *Montes et al. (2012)* suggested that deformation in the Isthmus resulted from opposite vertical-axis rotations on both sides of the Rio Gatun Fault. The Isthmus can be classifed as an orocline because it is a curved orogen in map view, that has been

bent about a vertical axis of rotation (*Johnston et al., 2013*). Block rotation and fragmentation are recorded by older arc segments, whereas younger segments are less deformed. This provides a clear chronology of deformation of the arc, where arc shut down at ~38 Ma may be marking the initiation of arc fragmentation and oroclinal bending. Deformation occurred in three main stages with large and moderate rotations. In the first stage, counterclockwise rotations took place between 38 and 28 Ma, additionally to left-lateral strike-slip of the arc. In a second stage, between 28 and 25 Ma clockwise rotations of the central arc segments took place. Finallly, the orocline tightenining happened after 25 Ma (*Montes et al., 2012*).

2.2. Azuero Peninsula

The Azuero Peninsula is located in the Panamanian forearc along the southwestern edge of the Caribbean Plate (*Buchs et al., 2011*; Fig. 1). The Azuero Peninsula is composed by a volcanic basement that has been intruded by arc and protoarc sequences, has experienced seamount accretion, and is overlain by forearc sediments.

Large structural and tectonic features have been mapped in the Azuero Peninsula: The Azuero Soná Fault Zone, the Central Coiba Fault Zone, the South Coiba Fault Zone, all of these with high angle dips, and with left-lateral strike-slip motion since Pliocene times (*Mann and Corrigan, 1990*; *Mann and Kolarsky, 1995*; *Kolarsky et al., 1995*). Additionally, there are other features as the Ocu-Parita Fault Zone and the Joaquin Fault Zone (*Buchs et al., 2011*; *Corral et al., 2013*; *Guidice and Recchi, 1969*; *Kolarsky et al., 1995*). The most important structure is the Azuero Soná Fault Zone, as a shear zone with incohesive brittle, cohesive brittle and narrow ductile rocks. Ductile deformation markers within the fault zone preliminarily suggest a dextral sense of shear for the fault, with a normal displacement along a plane coincident with foliation dipping at 60 degrees to the southwest in average, aligned with the overall strike of the fault zone (*Pérez-Angel, 2015*).

Buchs et al. (2010, 2011a,b) divided the Peninsula into four tectonostratigraphic units: The Azuero Marginal Complex, the Azuero Mélange, the Azuero Accretionary Complex and the overlapping sequences. These can be roughly summarized as an autochthonous Marginal Complex where the basament is composed by the Azuero Plateau intruded by arc sequences (the arc and proto-arc groups). The allochthonous part is found south of the Azuero Soná Fault Zone, and is composed of accreted seamounts separated from the marginal complex by a mélange zone (Azuero Accretionary Complex and the Azuero Mélange). Overlapping sequences are suggested to be non-conformably covering this complex geological arrangement.

Within this complex geological arrangement, bedded basalt flows interbeded with hemipelagic limestone or mudstone in the Marginal Complex provide paleomagnetic sampling targets. These bedded sequences have been correlated with the Upper Cretaceous Ocu Formation overlapping plateau basement (*Buchs et al., 2010*; *Corral et al., 2011*; *Lissinna, 2005*). These sequences are composed of gray to white, fine-grained limestones, interbedded with tuffs, and lava flows, collectivelly more than 1500-m thick (*Corral et al., 2011*; *Guidice and Recchi, 1969*; *Kolarsky et al., 1995*). They are cross-cut by basaltic dikes (*Buchs et al., 2010, 2011*; *Wegner et al., 2011*). Younger sequences overyling these deposits lack layering that can be used as paleohorizontal reference.

Within the accreted seamount province, layered and pillow basalts also provide opportunity for paleomagnetic sampling. The seamounts are composed of massive and

pillow lavas, sheeted lava flows, basaltic breccias and subaerial lava flows. These are also cross-cut by basaltic dikes (*Buchs et al., 2011*; *Hoernle et al., 2002*; *Hoernle and Hauff, 2007*).

Buchs et al. (2011b) and *Mann and Corrigan (1990)* have described the Azuero Soná Fault Zone as the boundary that separates a volcanic arc basement in the north part of the Azuero Peninsula from a basaltic basement in the south; in other words, Azuero Soná Fault Zone represents the boundary between the authocthonous and the allocthonous terranes. However, preliminary field, petrological and geophysical studies (*Agudelo-Mota, 2016*; *Ayala, 2015*; *Jara, 2016*; *Revelo, 2015*; *Urdaneta, 2016*) suggest that the limit between authochtonous and allochthnous terranes is located father south, within what *Buchs et al. (2011b)* considers the Azuero Mélange. Also, sedimentary successions overlapping basement rocks in both regions, have been reported faulted within the Azuero Soná Fault Zone (*Garzon, 2016*; *Gongora, 2016*; *Ortiz-Guerrero, 2016*).

Previous paleomagnetic studies performed in the peninsula (*Di Marco et al., 1995*; *Frisch et al., 1992*) have shown vertical-axis rotations close to 100° and inclination values indicating equatorial positions. *Frisch et al. (1992)* studied 4 sites in the Azuero Peninsula, on lava flows and a dike from Cenozoic units (Paleocene and Miocene), nonetheless paleomagnetic directions yielded from these 4 sites were too scattered. *Di Marco et al. (1995)* investigated two sites in the same area on calcareous beds interbedded in volcanic arenites from the Güera Formation. These sites showed an east shallow direction and positive fold test, so an equatorial paleoposition and clockwise vertical-axis rotations about 60° seemed confirmed. However as all the units sampled are Cretaceous in age, and a tectonic reconstruction of the terrrane could not be performed. In conclusion, the tectonic evolution of the Azuero Peninsula has not been interpreted by paleomagnetic data because the reliable data available is scarce and constrained just to Cretaceous units.

3. METHODOLOGY

Two hundred and forty oriented cores from twenty-five sites (Table 1) were collected in the southwestern part of the Azuero Peninsula. Most cores (210) were collected using a portable gasoline-powered drill and a copper orienter. Other cores (30) were collected from oriented hand samples with a static drill and cut to the standard 2.4 cm diameter by 2 cm long in the laboratory. At least nine cores were taken at each site. We performed two field tests (dike and conglomerate test) to determine relative age of magnetization. The 25 sites were divided into four blocks (Table 1) according to stratigraphy, age and distance between sites. The structure that divided the main two groups is the Azuero Soná Fault Zone, because initial hypothesis suggested that this structure was the most relevant structural boundary in the peninsula. The laboratory analysis were carried out at Instituto de Geociencias Básicas, Aplicadas y Ambientales de Buenos Aires (IGEBA) of the Universidad de Buenos Aires, Argentina. Demagnetization cleaning processes were conducted by alternating fields (AF) and high temperatures (HT) methods (*Butler, 1992*) with an AGICO LDA5 AF demagnetizer and an ASC TD48-SC thermal specimen demagnetizer and the magnetic remanence was measured in a AGICO JR-6 spinner magnetometer or a 2G cryogenic magnetometer. To decide on the best magnetic demagnetization procedure for each site, we performed a pilot test in all sites.

Table 1. Summary of the paleomagnetic sites.

Block	Site	Lat. N [°]	Long. W [°]	Number of Cores	Lithology	Age
Discarded	Oc01	7.59973	–80.9740	7	Sandstone	Camp.-Maastr.
Ocú	Oc02	7.63059	–80.9290	10	Basalt	Camp.-Maastr.
Ocú	Oc03	7.63032	–80.9273	9	Basalt	Camp.-Maastr.
Ocú	Oc04	7.62767	–80.9273	12	Basalt	Camp.-Maastr.
Ocú	Oc05	7.63147	–80.9327	11	Conglomerate	Camp.-Maastr.
Ocú	Oc06	7.63011	–80.9296	11	Dike	Camp.-Maastr.
Ocú	Oc07	7.62056	–80.9181	12	Tuffs	Camp.-Maastr.
Ocú	Oc08	7.62032	–80.9177	10	Basalt	Camp.-Maastr.
Ocú	Oc09	7.63023	–80.9295	8	Basalt	Camp.-Maastr.
Ocú	Oc10	7.62688	–80.9280	7	Basalt/biomicrite	Camp.-Maastr.
Discarded	H01	7.45479	–80.9022	5	Masive picrites	Paleocene-Eocene
Honda	H02	7.45479	–80.9022	9	Basalt	Paleocene-Eocene
Honda	H03	7.45498	–80.8783	9	Basalt	Paleocene-Eocene
Honda	H04	7.45965	–80.8937	11	Basalt	Paleocene-Eocene
Honda	H05	7.46557	–80.8650	8	Basalt	Paleocene-Eocene
Honda	H06	7.47237	–80.9306	7	Pillow basalts	Paleocene-Eocene
Honda	H07	7.46964	–80.8362	13	Basalt	Paleocene-Eocene
Honda	H08	7.47806	–80.8630	10	Pillow basalts	Paleocene-Eocene
Discarded	V01	7.41164	–80.8364	10	Pillow basalts	Paleocene-Eocene
Varadero	V02	7.29846	–80.8685	6	Amigdular and vesicular basalt	Paleocene-Eocene
Varadero	V03	7.30125	–80.8586	8	Amigdular and vesicular basalt	Paleocene-Eocene
Varadero	V04	7.30397	–80.8563	9	Amigdular and vesicular basalt	Paleocene-Eocene
Pachotal	P01	7.32902	–80.8952	7	Vesicular basalt	Eocene
Pachotal	P02	7.32872	–80.8969	10	Mudstone	Eocene
Pachotal	P03	7.45498	–80.8782	4	Mudstone	Eocene

* The age of all sites was taken from *Buchs el at. (2011b)*, the only data avaliable in the literature.

Demagnetization steps for alternating fields were as follows: 0, 2, 4, 6, 8, 10, 15, 20, 25, 30, 40, 50, 60,70 and/or 80 mT, and steps for thermal demagnetization as follows: 0, 100, 150, 200, 250, 300, 350, 400, 450, 500, 525, 550 and 575°C.

We analyzed the paleomagnetic data using RemaSoft 3.0 software (*Chadima and Jelínek, 2009*), and isolated a characteristic paleomagnetic component (ChRM) for each sample applying the means of principal component analysis (PCA) (*Kirschvink, 1980*). We employed orthogonal demagnetization or Zijderveld diagrams in the analysis of principal components. Mean magnetization directions were calculated using Fisher's statistics (*Fisher, 1953*), and in the most cases we used seven or more samples for each site.

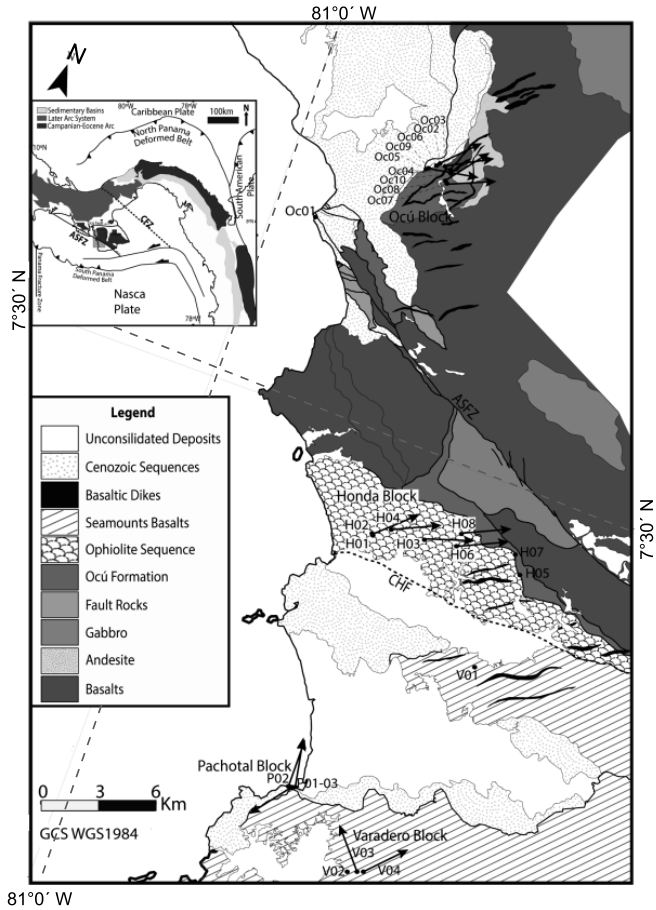

Fig. 1. Geologic map of the Azuero Peninsula (modified from *Ortiz-Guerrero, 2016*) with localization of all paleomagnetic sites and the main structures in the area: Azuero Soná Fault Zone (ASFZ) and Cerro Honda Fault (CHF), and general tectonic configuration of theIsthmus of Panama: Canal Fracture Zone (CFZ).

4. RESULTS

Sampled sites were grouped into four fault-bounded blocks according to field relations and with the purpose of developing a tectonic interpretation (Fig. 1). Ten sites were sampled in the Ocú block, eight in the Honda block, four in Varadero block and three in the Pachotal block (Table 1). We took advantage of layered basalt flows and interbedded fine-gained sedimentary rocks for tilt corrections, assuming that deposition was nearly horizontal. The statistical values as precision parameter k and confidence angle α_{95} (*Fisher, 1953*), and the demagnetization ranges are reported for each site (Table 2).

Table 2. Mean-site directions of characteristic paleomagnetic components for all sites, the data are divided into two parts: sites used in the final analysis with good statistical support; and discarded data due to statistical problems or remagnetization evidence. BTC and ATC: before and after tilt correction, respectively. *N*: number of specimens or sites analysed, *n*: number of specimens used in statistics. α_{95} and *K*: 95% confidence angle and precision parameter (*Fisher, 1953*). * Conglomerate test site; ** Baked contact test site.

Site	Bedding		*N*	*n*	Demag. Range		BTC		ATC		α_{95} [°]	*K*
	Dip [°]	Dip Direction [°]			AF [mT]	Thermal [°C]	*Dec* [°]	*Inc* [°]	*Dec* [°]	*Inc* [°]		
Sites used in the final analysis												
Oc02	45	294	15	8	2–80	100–550	61.9	–18.6	64.4	10.7	13.9	16.91
Oc03	54	290	12	10	2–60	100–550	92.1	–62.1	100.1	–16.9	4.8	103.44
Oc05*	---	---	13	12	2–60	100–550	---	---	---	---	52.1	1.66
Oc06**	47	287	15	15	2–60	100–550	40.1	–18.5	46.1	3.2	10.0	19.94
Oc07	31	326	15	6	2–60	100–550	75.5	–28.2	86.8	–14.7	11.6	34.14
Oc08	31	326	13	7	2–60	100–550	46.0	–20.8	58.8	–22.9	13.8	20.22
Oc09	40	266	11	9	2–80	100–550	260.1	38.2	81.3	1.7	4.2	150.13
Ocú Block			**5**		**2–80**	**100–550**	**69.6**	**–34.5**	**78.4**	**–8.2**	**20.8**	**15.54**
H02	22	189	14	7	2–60	100–575	62.3	8.7	67.2	21.2	8.1	56.69
H03	18	120	9	5	2–60	100–575	86.2	1.8	85.2	–13.0	13.2	34.70
H04	66	181	21	19	2–60	100–575	97.6	–1.1	92.7	–6.5	3.9	75.70
H06	26	349	10	7	2–60	100–575	83.1	–6.9	85.7	–4.4	10.0	37.31
H08	16	230	13	7	2–60	100–550	266.2	0.9	87.1	11.9	11.0	31.00
Honda Block			**5**		**2–60**	**100–575**	**83.2**	**0.3**	**83.8**	**1.8**	**16.5**	**22.85**
Ocú+Honda Blocks			**10**		**2–60**	**100–575**	**77.2**	**–16.6**	**81.2**	**–3.2**	**11.7**	**18.09**

Table 2. Continuation.

Site	Bedding		N	n	Demag. Range		BTC		ATC		α_{95} [°]	K
	Dip [°]	Dip Direction [°]			AF [mT]	Thermal [°C]	*Dec* [°]	*Inc* [°]	*Dec* [°]	*Inc* [°]		
Sites used in the final analysis												
V03	9	340	4	4	2–60	---	339.4	10.6	339.4	1.6	13.0	50.84
V04	23	257	5	5	2–60	100–550	242.7	20.6	63.6	1.8	5.5	194.41
P01	19	119	7	6	2–80	100–550	352.3	40.2	9.1	49.4	11.8	33.22
P02	37	107	7	4	2–60	100–550	59.1	10.8	238.2	14.2	16.9	30.47
P03	40	103	4	3	2–60	---	20.3	1.5	19.6	-3.6	12.0	107.18
Discarded sites												
Oc01	7	170	2	0	2–60	100–575	---	---	---	---	---	---
Oc04	44	245	11	0	2–80	100–575	---	---	---	---	---	---
Oc10	49	6	8	5	2–60	100–550	11.9	29.7	11.5	–19.1	24.4	10.82
H01	21	163	8	6	2–60	100–575	224.5	–13.8	47.9	8.7	15.0	21.01
H05	48	212	8	8	2–60	100–575	74.2	34.4	123.1	56.4	4.1	187.31
H07	22	47	16	14	2–60	100–550	54.3	–27.3	56.9	–49.0	8.0	25.56
V01	15	201	14	9	2–60	100–550	168.21	–29.2	161.8	–41.3	38.4	2.76
V02	21	31	5	5	2–60	---	261.5	27.7	273.2	39.5	65.8	2.31

4.1. Ocú block

A total of ten sites (Table 1) were collected in the north area of the Peninsula, along the Palo Seco river and the Naranjo creek (Fig. 1). Seven of these sites were drilled from basalt-limestone interbeds of the Ocú Formation, Upper Cretaceous age, one from tuffs which are the basement of the Ocú Formation, one from a Cenozoic basal conglomerate and one from a dike crosscutting the Ocú Formation. A main component (Fig. 2a) was isolated at temperatures from 100 to 550°C or with highest alternating field from 20 to 60 or 80 mT (Fig. 2b). Two sites (Oc01 and Oc04) showed high scattering in the demagnetization sequence, thus their components were not calculated. Directional dispersion was high for ChRM at site Oc10 and also was excluded from computing the final results (Table 2). The characteristic components in Ocú Block showed declination values oriented to the east and northeast (between 100.1 ± 4.8° and 58.8 ± 13.8°, after tilt correction) which suggests large vertical-axis rotations, with low values of positive and negative inclinations (Table 2) that decreased with the tilt correction (Fig. 2c). The final mean direction for this block was calculated (Table 2 and Fig. 2c) and show increase in the clustering of data after tilt correction. Also, one direction in the block is to the west, so timing of magnetization must cover two chrons of magnetic polarity (Table 2).

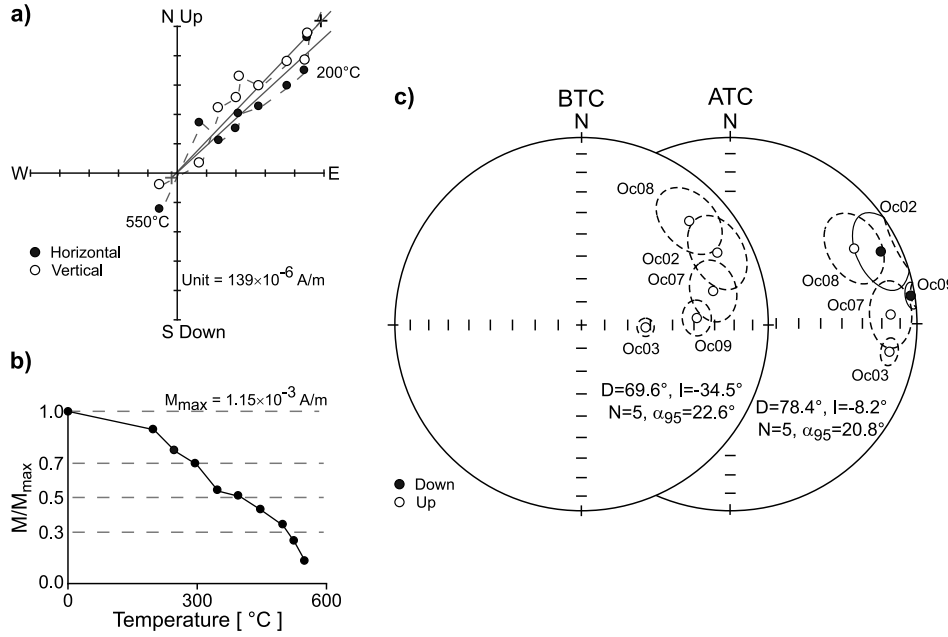

Fig. 2. Representative examples (Site Oc03-4a) of **a)** Zijderveld diagram and **b)** normalized natural remanent magnetization (*NRM*) decay measured on Ocú block. **c)** Equal area plots for the mean directions of each site of the block, all values were projected to the east. BTC - before tilt correction; ATC - after tilt correction; *D* and *I* - declination and inclination of the mean direction of the block; *N* - number of sites; α_{95} - confidence angle (*Fisher, 1953*).

Conglomerate test

The conglomerate test for site Oc05 was carried out in the Palo Seco river (Fig. 1) in a basal conglomerate that separates unconformably the Cenozoic sequences from the Ocú Formation. Eleven cores were drilled, each one in a different pebble of the conglomerate. This fining-upward conglomerate is composed by a lithic sand matrix with rounded basaltic fragments of a large range of sizes (from pebbles to boulders; 2–500 mm). For this site, the main component (Fig. 3a) was isolated at temperatures between 100 and 550°C and from 20 to 60 mT in AF (Fig. 3b). We found large scattering among the components calculated ($\alpha_{95} = 52.1°$, Fig. 3c) suggesting a positive conglomerate test, which means that the ChRM was acquired prior to the accumulation of the conglomerate.

Baked contact test

The baked contact test was carried out in the Palo Seco river too (Fig. 1), in a basaltic dike that crosscuts the Ocú Formation. Eleven cores were drilled in the diabase dike (site Oc06) and seventeen in the basalts that belong to the sites Oc03 and Oc09, with maximum separation of the dike of ~130 m. Site Oc03 was closer to the dike than site Oc09 to investigate the possible influence of the dike in a remagnetization process. In most specimens a ChRM was calculated. The component (Fig. 3d) was isolated at temperatures between 100 and 550°C and from 20 to 40–60 mT for the dike and 80 mT in the host rock (Fig. 3e).

The declination values for the dike showed a northeastern orientation (46.1 ± 10°) (Table 2), instead the values for the host rock showed an eastern orientation (100.1 ± 4.8° and 81.3 ± 4.2°) (Table 2). The inclination values for the dike were between low and moderate (–18.5°), for the host rock instead these were large (–62.1° and 38.2°) before tilt correction; however, with the tilt correction all of them decreased (3.2°, –16.9° and 1.7°, respectively) (Table 2). Inclinations for the dike and host rocks are clearly different in situ but almost identical after tilt correction (Fig. 3f–g). In conclusion, the baked contact test yielded a result that is not conclusive but points to a pre-tectonic age for the magnetization of both the dike and the Ocú Formation, which is consistent with the results of the conglomerate test. This suggests that ChRM of the dyke and host rocks were acquired a different time, and the intrusion event related to the dyke did not affect directions of nearby sites Oc03 and Oc09.

4.2. Honda block

The Honda block, located south of the Azuero Soná Fault Zone, was sampled at eight sites distributed in different creeks (Fig. 1 and Table 1). The sequences sampled in this block are monotonous interbedding of basalt flows, vesicular basalts, massive picrites, pillow basalts and occasional mudstone and chert intercalations. In most sites of the block it was possible to determine a characteristic component of remanent magnetization in temperatures from 100 to 575°C or from 20 to 60 mT in AF (Fig. 4a,b). However, three sites (H01, H05 and H07) were ruled out because they showed high directional scattering or unstable performance, which is possibly explained by its proximity to the Azuero Soná Fault Zone (Fig. 2). We find a characteristic paleomagnetic component in this block with

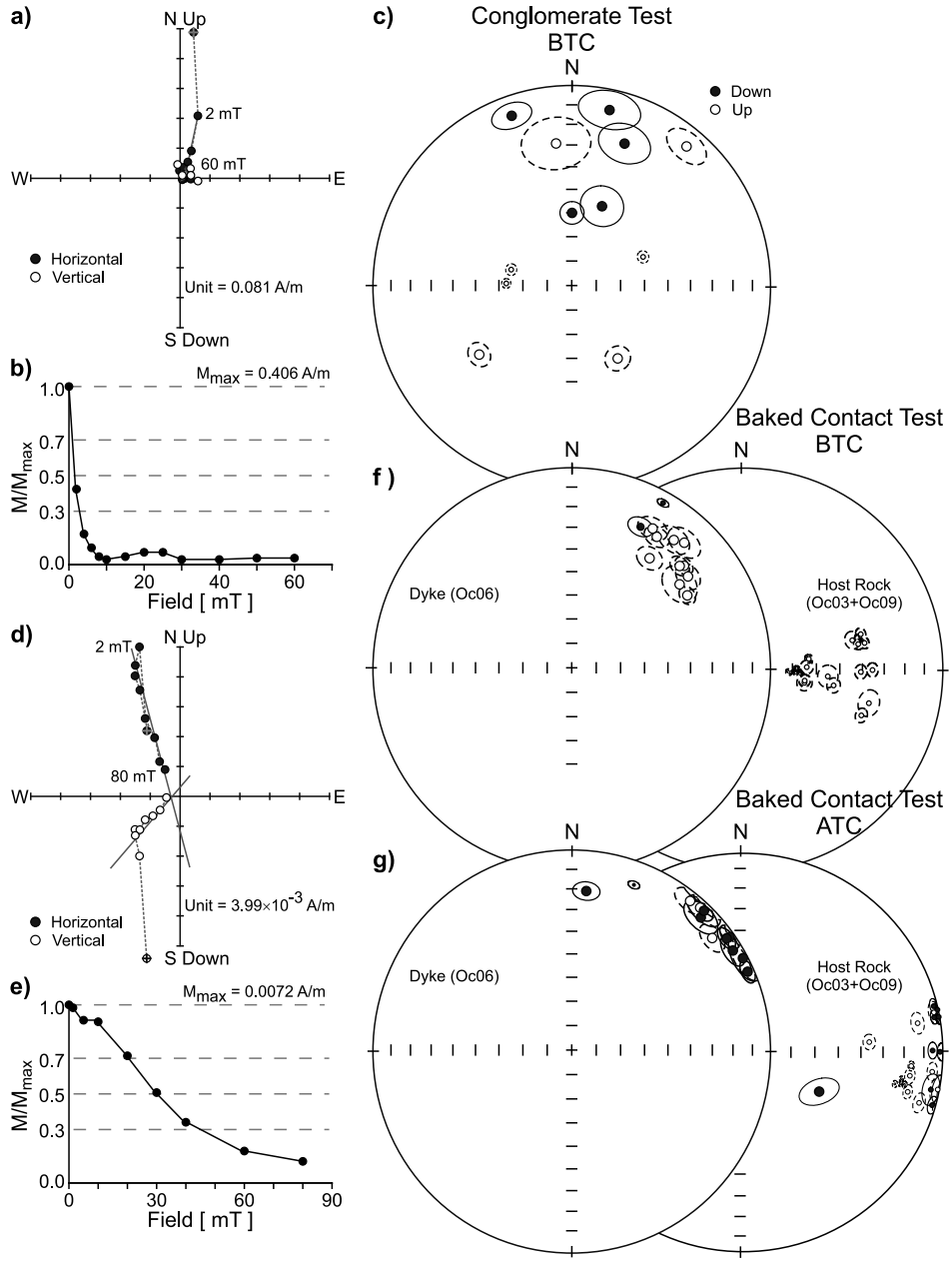

Fig. 3. **a)** Representative Zijderveld diagram (Site Oc05-6a); **b)** representatiove plot of *NRM* decay (Site Oc05-6a), evaluated after conglomerate test; **c)** equal area plots of the mean directions after conglomerate test (note that all the components are scattered); **d)** and **e)** the same as in a) and b), respectively, but for the Site Oc03-9a and baked contact test; **f)** and **g)** equal area plots of the mean directions after baked contact test. BTC - before tilt correction; ATC - after tilt correction.

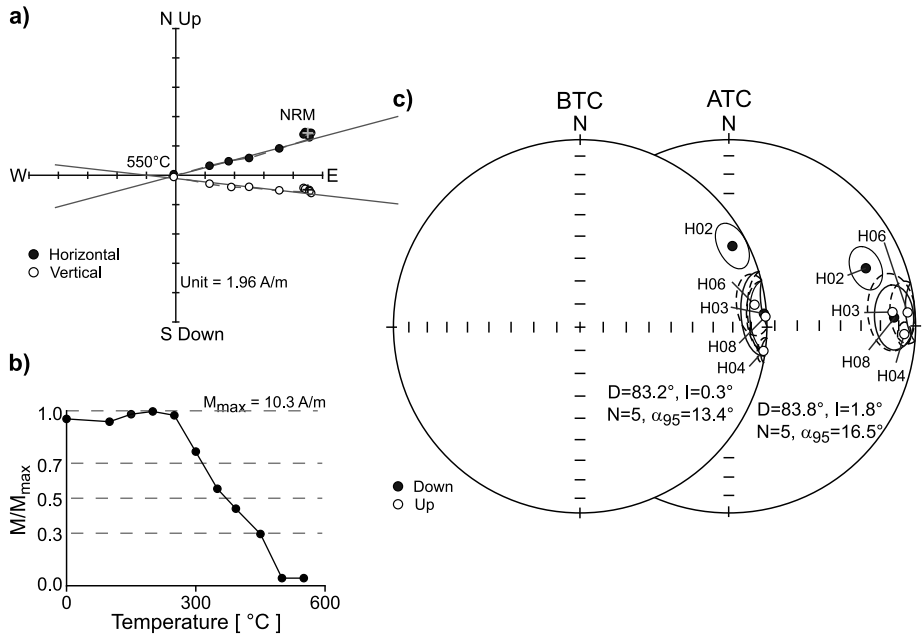

Fig. 4. The same as in Fig. 2, but for Honda block (Site H08-5b).

high values of declination (between 92.7 ± 3.9° and 67.2 ± 8.1°, after tilt correction) (Fig. 4c), that suggest large tectonic rotations, with low and moderate values of positive and negative inclinations (Table 2). The final mean direction for this block was calculated (Table 2 and Fig. 4c) and does not show significant change in the clustering of data before and after tilt correction. Also as in Ocú Block, one direction in the block is to the west, so timing of magnetization must cover two chrons of magnetic polarity (Table 2).

4.3. Varadero block

Four sites were collected in the accretionary complex exposed in the Varadero Block. Varadero corresponds to the southernmost part of the peninsula (*Buchs et al., 2011b*). The lithology in the area is dominated by amygdular and vesicular basalts with evidence of flow alignment in the vesicles. In the paleomagnetic analysis of this area, it was possible to determine a characteristic paleomagnetic component for each site (Fig. 5a), isolated at temperatures from 100 to 550°C or at fields from 20 to 60 and 80 mT (Table 2, Fig. 5b). The sites V01 and V02 have high values of α_{95} (38.4° and 65.8°, respectively) so they were not used. Additionally, mean paleomagnetic directions for the other two sites (V03 and V04) were not consistent (Fig. 5c) preventing to compute a valid mean direction for the block.

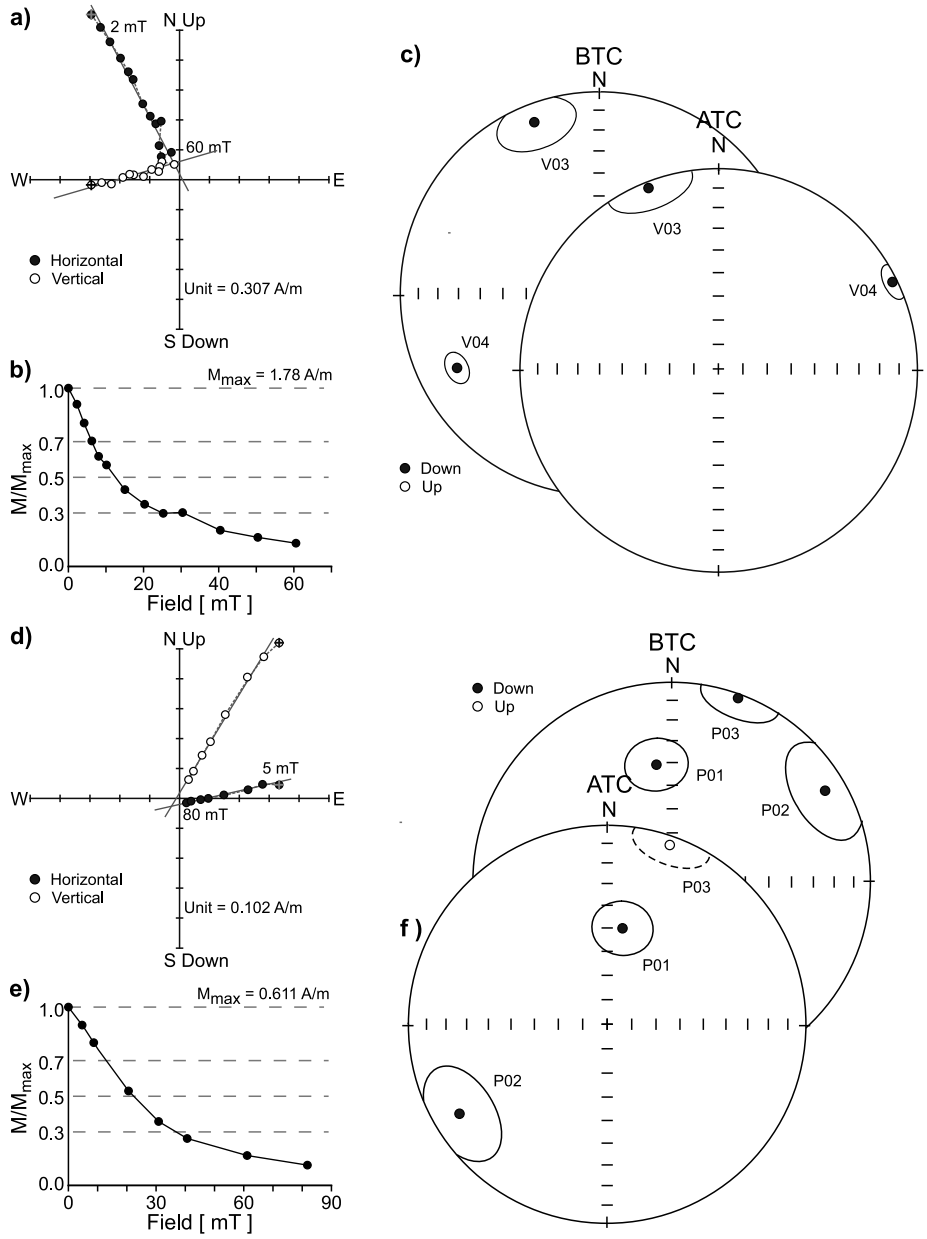

Fig. 5. **a)** Representative Zijderveld diagram (Site V03-3a); **b)** representatiove plot of *NRM* decay (Site V03-3a), and **c)** equal area plots of the mean directions of each site at the Varadero block; **d) – f)** the same for the Pachotal block, respectively (Site P01-6a in d) and e)). BTC - before tilt correction; ATC - after tilt correction. The site P01 may represent the most recent event of magnetization.

4.4. Pachotal block

We performed sampling at three sites in Pachotal area (Fig. 1), in different beds from diverse lithologies, as vesicular basalts and mudstones from the Covachón Formation of Eocene or younger age. The principal component reported in the Zijderveld diagrams (Fig. 5d) for these sites was isolated from 100 to 600°C or 20 to 60 mT (Fig. 5e). A reliable mean paleomagnetic direction could be determined for each site, but it was not possible to calculate a mean direction for the entire block due to large between-site dispersion. Additionally, paleomagnetic direction uncovered in the P01 may represent the present magnetic field (Fig. 5f).

5. DISCUSSION

The paleomagnetic data presented above indicate that the characteristic paleomagnetic components isolated in the western Azuero peninsula might be the record of primary magnetization components. Once placed in a spatial frame, it is clear that these primary components define two domains: one with consistently large vertical-axis rotations to the north, and another with scattered paleomagnetic components to the south. Firstly, the unblocking temperatures around 500–550°C and AF destructive fields in the range of 20–60 mT points to (Ti-poor)magnetite as the main remanence carrier in the study rocks. Futhermore, the conglomerate test indicates that magnetic components in the Campanian to Maastrichtian basaltic sequences were acquired before accumulation of Eocene clastic sequences, and there are no remagnetization events of Eocene or younger age in the western Azuero peninsula (Fig. 3c). The baked contact test, performed in a large diabase dike intruding the calcareous/basaltic Ocú Formation (Figure 3f-g) also suggests that intrusion of basaltic magmas, of likely Paleonece age, did not reset the paleomagnetic signature of the directions isolated in the Upper Cretaceous Ocú Formation.

Secondly, paleomagnetic data obtained for the northern Ocú and Honda blocks separated by the Azuero Soná Fault Zone-reveal large vertical-axis rotations with similar inclination and declination values (Figs 2c and 4c, Table 2). Figure 6 illustrates the mean site directions from Cretaceous and Paleocene rocks sampled at these two blocks, which show a much better directional consistency after tilt correction, futher supporting the primary nature of the characteristic remanence. Given the lithological and paleomagnetic similarity, we grouped primary paleomagnetic components of the Ocú and Honda blocks to obtain a single mean direction of declination $D = 77.2°$ and inclination $I = -16.5°$ ($\alpha_{95} = 16.5°$ and $k = 9.51$) before tilt correction and $D = 81.2°$ and $I = -3.2°$ ($\alpha_{95} = 11.7°$ and $k = 18.09$) after tilt correction (Fig. 6). Assuming that the expected declination value for Azuero Peninsula (7°N, 80°W) is $7.79 \pm 2.7°$ respect to the paleomagnetic pole of 70 Ma for the South American Craton of *Torsvik (2008)*, the magnitude of rotation is $73.4 \pm 12°$, the rotation was computed in reference to South American Craton because the Caribbean Plate has not paleomagnetic poles at this age. Futhermore, we calculated expected declination values for different ages (Fig. 6) for supporting the consistency of the data obtained. The clockwise sense of rotation was inferred by the configuration of the arc. A clockwise rotation is kinematically more plausible if the southern edge of the Azuero plateau face Galapagos-derived seamounts (*Buchs et al., 2011a*; *Gazel et al.,*

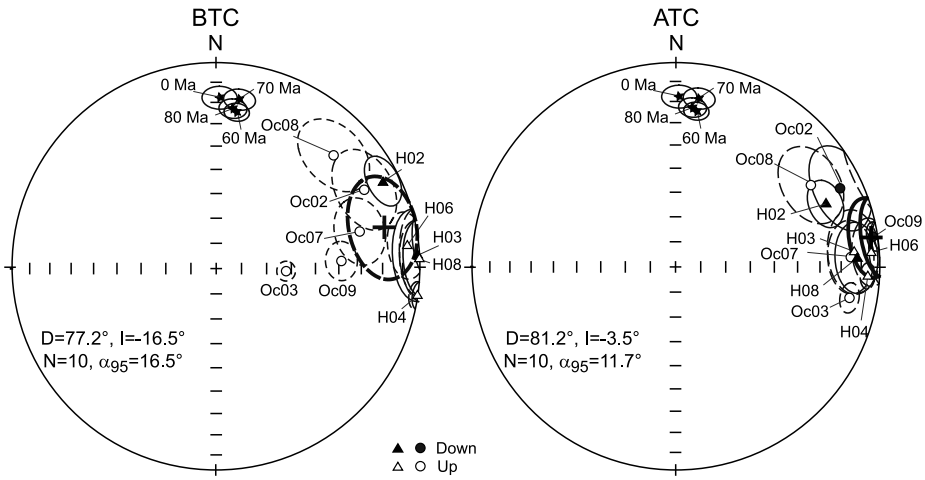

Fig. 6. Combined mean direction of characteristic component for Ocú (circles) and Honda (triangles) blocks. BTC - before tilt correction; ATC - after tilt correction; *D* and *I* - declination and inclination of mean directions of the block; *N* - number of sites; α_{95} - confidence angle (*Fisher, 1953*). Stars represent the expected directions for Azuero Peninsula (7°N, 80°W) using the paleomagnetic poles of *Torsvik (2008)* for South American Craton.

2009; *Trela et al., 2015*) before rotation takes place. An opposite sense of rotation (with a larger magnitude) would instead place the edge of the plateau facing away from the Galapagos hotspot. The components marking a large vertical-axis rotation isolated in Azuero, however, force a southward bend (Fig. 7) in the Campanian to Eocene arc system of *Montes et al. (2012)*.

Finally, the uniformity of paleomagnetic components across the Azuero Soná Fault Zone (Ocú and Honda blocks, Fig. 6) suggests that this fault does not separate tectonic domains. Instead, the Cerro Honda Fault (Fig. 1) located to the south, is more likely to represent a suture between the Azuero plateau and far travelled seamounts. Southern blocks (Varadero and Pachotal) show scattered paleomagnetic components (Table 2) consistent with the interpretation that southern Azuero peninsula is in fact composed of several distinct seamounts (*Buchs et al., 2011a*). Collision and dismemberment of seamounts carrying different paleomagnetic direction values, would be recorded as blocks with scattered paleomagnetic components (Fig. 5).

The discussion of the paleomagnetic data presented above can be used to refine the paleogeographic model for the Campanian-Eocene arc (*Montes et al., 2012*). When 73.4° clockwise vertical-axis rotation are subtracted from the arc segment preserved in the Azuero peninsula, a northeast-trending arc segment results (Fig. 7), that should then connect with the west-northwest arc segments of the San Blas, Choco and Canal blocks at 38 Ma. Collision of Galapagos-derived seamounts (*Buchs et al., 2011a*; *Gazel et al., 2009*), would then drive deformation west of the Canal basin, probably causing rotation of the Azuero arc segment and left-lateral offset with respect to El Valle block. This interpretation is consistent with previos studies (*McCabe, 1984*; *Vogt et al., 1976*; *Wallace*

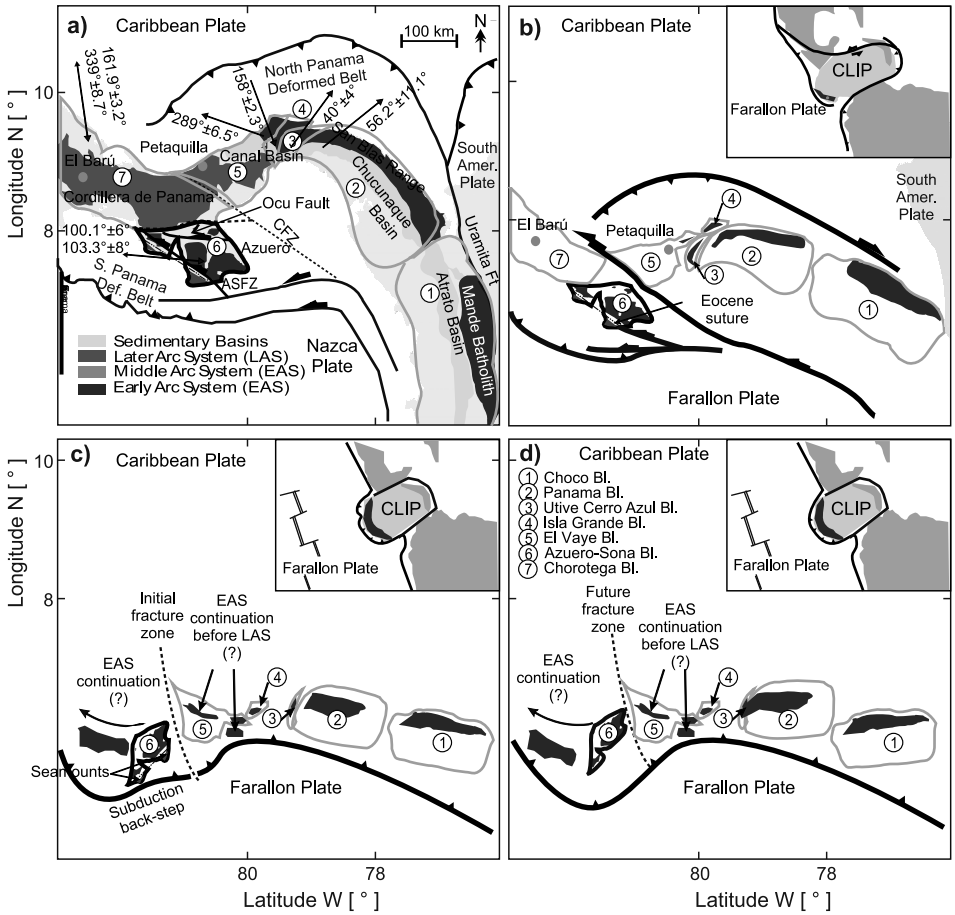

Fig. 7. Tectonic reconstruction model of Campanian to Eocene belt. Paleomagnetic data reported in this paper for Azuero Peninsula and *Montes et al. (2012)* for the other localities in the Panamanian Isthmus. **a)** Current configuration, **b)** reconstruction at 28 Ma, **c)** reconstruction at 45 Ma, and **d)** reconstruction at 70 Ma (modified from *Montes et al., 2012*). CLIP: Caribbean Large Igneous Province.

et al., 2005) showing that large-vertical axis rotations result from the collision between microblocks (e.g., seamounts) and oceanic arcs. *Wallace et al. (2005)* describe cases in the South Pacific where GPS measurements allow quantifying displacements and rotations resulting from these collisions.

6. CONCLUSIONS

Five conclusions can be derived from the data presented in this paper: 1) The paleomagnetic data in Azuero Peninsula show two different domains separated by Cerro

Honda Fault. One domain with large clockwise vertical-axis rotations (81.2 ± 11.7°), and another with scattered paleomagnetic components; 2) the ChRM isolated in Late Cretaceous Ocú Formation was previous to intrusion of basaltic dikes and deposition of Eocene clastic sequences; 3) Azuero Soná Fault Zone does not represent a major tectonic boundary for the tectonic blocks in the peninsula; 4) Using the restoration of paleomagnetic data in Azuero Peninsula suggest that WNW-ESE Campanian to Eocene arc proposed by *Montes et al. (2012)* had a northeast-trending segment in the Azuero block in late Cretaceous to Paleogene times; 5) The time of magnetization in the segment of the Azuero Peninsula in pre-Paleocene time, the arc was located near to the Equatorial magnetic line, supporting previous interpretations that consider the location of the Panama arc at the line of the magnetic equador.

Acknowledgments: This study has been made possible thanks to Uniandes P12.160422.002/001, PCP PIRE (Partnerships for International Research and Education) from University of Florida, Smithsonian Tropical Research Institute, Corrigan grant of Asociación Colombiana de Geólogos y Geofísicos del Petroleo (ACGGP). Thanks to Corporación Geológica Ares for lending field tools and the IGEBA of Universidad de Buenos Aires for allowing us to use their laboratory equipment. All the participants of the Geo Field Camp Uniandes 2014-2015 enthusiastically helped us in the field work. Finally, thanks to Edgar Cortés, Giovanny Jiménez, Avto Gogichaishvili and an anonymous reviewer for their comments and review of the manuscript.

References

Agudelo-Motta L.C., 2016. *Geochemical and Mineralogical Characterization of Mineralized Volcanic Sequences in Loma Iguana Region (Azuero Peninsula, Panama)*. Undergraduate Thesis. Universidad de los Andes, Bogotá, Colombia.

Ayala J., 2015. *Bouguer Anomaly Model of Western Azuero Peninsula, Panama*. Undergraduate Thesis. Universidad de los Andes, Bogotá, Colombia.

Buchs D.M., Arculus R.J., Baumgartner P.O., Baumgartner-Mora C. and Ulianov A., 2010. Late Cretaceous arc development on the SW margin of the Caribbean Plate: Insights from the Golfito, Costa Rica, and Azuero, Panama, complexes. *Geochem. Geophys. Geosyst.*, **11**, Q07S24, DOI: 10.1029/2009GC002901.

Buchs D.M., Arculus R., Baumgartner P. and Ulianov A., 2011a. Oceanic intraplate volcanoesexposed: Example from seamounts accreted in Panama. *Geology*, **39**, 335–338, DOI: 10.1130/G31703.1.

Buchs D.M., Baumgartner P.O., Baumgartner-Mora C., Flores K. and Bandini A.N., 2011b. Upper Cretaceous to Miocene tectonostratigraphy of the Azuero area (Panama) andthe discontinuous accretion and subduction erosion along the Middle Americanmargin. *Tectonophysics*, **512**, 31–46, DOI: 10.1016/j.tecto.2011.09.010.

Camacho E., Hutton W. and Pacheco J., 2010. A new look at evidence for a Wadati-Benioffzone and active convergence at the North Panama Deformed Belt. *Bull. Seismol. Soc. Amer.*, **100**, 343–348, DOI: 10.1785/0120090204.

Chadima M. and Hrouda F., 2006. Remasoft 3.0 a user-friendly paleomagnetic data browser and analyzer. *Travaux Géophysiques*, **XXVII**, 20–21.

Coates A.G. and Obando J.A., 1996. The geologic evolution of the Central American isthmus. In: Jackson J.B.C., Budd A.F. and Coates A.G. (Eds), *Evolution and Enviroment in Tropical America*. University of Chicago Press, Chicago, IL, 21–56.

Corral I., Gómez-Gras D., Griera A., Corbella M. and Cardellach E., 2013. Sedimentationand volcanism in the Panamanian Cretaceous intra-oceanic arc and fore-arc: New insights from the Azuero Peninsula (SW Panama). *Bull. Soc. Geol. Fr.*, **184**, 35–45.

Corral I., Griera A., Gómez-Gras D., Corbella M., Canals A., Pineda-Falconett M. and Cardellach E., 2011. Geology of the Cerro Quema Au-Cu deposit (Azuero Peninsula, Panama). *Geol. Acta*, **9**, 481–498, DOI: 10.1344/105.000001742.

Di Marco G., Baumgartner P.O. and Channell J.E., 1995. Late Cretaceous-early Tertiary paleomagnetic data and a revised tectonostratigraphic subdivision of Costa Rica and western Panama. *Geol. Soc. Amer. Spec. Pap.*, **295**.

Duque-Caro H., 1990. Neogene stratigraphy, paleoceanography and paleobiogeography in northwest South America and the evolution of the Panama Seaway. *Palaeogeogr. Palaeoclimatol. Palaeoecol.*, **77**, 203–234, DOI: 10.1016/0031-0182(90)90178-A.

Fan G.W., Beck S.L. and Wallace T.C., 1993. The seismic source parameters of the 1991 Costa Rica aftershock sequence: Evidence for a transcurrent plate boundary. *J. Geophys.*, **98**, 15759–15778, DOI: 10.1029/93JB01557.

Fisher R.A., 1953. Dispersion on a sphere. *Proc. R. Soc. London A*, **217**, 295–305.

Garzon S., 2016. *Stratigraphy and Provenance of Cenozoic Sequences in the Panamanian Forearc*. Undergraduate Thesis. Universidad de los Andes, Bogotá, Colombia.

Gazel E., Carr M.J., Hoernle K., Feigenson M.D., Szymanski D., Hauff F. and van den Bogaard P., 2009. Galapagos-OIB signature in southern Central America: Mantle refertilization by arc-hot spot interaction. *Geochem. Geophys. Geosyst.*, **10**, Q02S11, DOI: 10.1029/2008GC002246.

Gongora D.E., 2016. *Sedimentological Analysis and Petrographic Characterization of the Sequences Outcropping in Torio and Palo Seco Beaches in the Azuero Peninsula, Panamá*. Undergraduate Thesis. Universidad de los Andes, Bogotá Colombia.

Guidice D. and Recchi G., 1969. *Geología del area del proyecto minero de Azuero*. Report, 48 pp. Programa para el desarrollo de las Nac. Unidas. Panama City, Panama.

Hoernle K. and Hauff F., 2007. Oceanic igneous complexes. In: Bundschuh J. and Alvarado G.E. (Eds), *Central America: Geology, Resources and Hazards*. Volume 1. CRC Press, Boca Raton, FL, 523–547.

Hoernle K., van den Bogaard P., Werner R., Lissina B., Hauff F., Alvarado G. and Garbe-Schönberg D., 2002. Missing history (16–71 Ma) of the Galapagos hotspot: Implications for the tectonic and biological evolution of the Americas. *Geology*, **30**, 795–798, DOI: 10.1130/0091-7613(2002).

Jara N.A., 2016. *2D Resistivity Characterization of Alluvial Deposits near Azuero Fault, Panama*. Undergraduate Thesis. Universidad de los Andes, Bogotá, Colombia.

Johnston S.T., Weil A.B. and Gutiérrez-Alonso G., 2013. Oroclines: thick and thin. *Geol. Soc. Am. Bull.*, **125**, 643–663, DOI: 10.1130/b30765.1.

Kesler S., 1978. Metallogenesis of the Caribbean region. *J. Geol. Soc. London*, **135**, 429–441.

Kirschvink J.L.,1980. The least-squares line and plane and the analysis of paleomagnetic data. *Geophysi. J. Int.*, **62**, 699–718.

Kolarsky R.A., Mann P., Monechi S., Meyerhoff H.D. and Pessagno Jr. E., 1995. Stratigraphic development of southwestern Panama as determined from integration of marine seismic data and onshore geology. *Geol. Soc. Am. Spec. Pap.*, **295**, 159–200.

Lissinna B., 2005. *A profile through The Central American Landbridge in Western Panama: 115 Ma interplay between the Galapágos Hotspot and the Central American Subduction Zone*. PhD Thesis. Kiel University, Kiel, Germany.

McCabe R., 1984. Implications of paleomagnetic data on the collision related bending of island arcs. *Tectonics*, **3**, 409–428.

Mann P. and Corrigan J., 1990. Model for late Neogene deformation in Panama. *Geology*, **18**, 558–562.

Mann P. and Kolarsky R.A., 1995. East Panama deformed belt: Structure, age, and neotectonic significance. *Geol. Soc. Am. Spec. Pap.*, **295**, 111–130.

Molnar P. and Sykes L., 1969. Tectonics of the Caribbean and Middle America regions from focals mechanisms and seismicity. *Geol. Soc. Am. Bull.*, **80**,1639–1684.

Montes C., Bayona G., Cardona A., Buchs D., Silva C., Morón S., Hoyos N., Ramírez C.A., Jaramillo C.A. andValencia V., 2012. Arc-continent collision and orocline formation: Closing of the Central America seaway. *J. Geophys. Res.*, **177(B4)**, B04105, DOI: 10.1029 /2011JB008959.

Ortiz-Guerrero C., 2016. *Tectonostratigraphic Reconstruction of the Azuero Peninsula; Geologic Mapping and Structural Cross-Sections*. Undergraduate Thesis. Universidad de los Andes, Bogotá, Colombia (https://documentodegrado.uniandes.edu.co/documentos/9649.pdf).

Pennington W., 1981. Subduction of the Eastern Panama Basin and Seismotectonics of Northwestern South America. *J. Geophys. Res.*, **86(B11)**, 10753–10770.

Pérez-Angel L.C., 2015. *Structural Characterization of the Azuero-Sona Fault Zone*. Undergraduate Thesis. Universidad de los Andes, Bogotá, Colombia.

Pindell J. and Kennan L., 2009. Tectonic evolution of the Gulf of Mexico, Caribbean and northern South American in the mantle reference frame: an update. *Geol. Soc. London Spec. Publ.*, **328**, 1–55.

Revelo B., 2015. *Use of Electromagnetic Geophysical Methods for Detecting Neotectonic Structures in the Azuero Peninsula, Panama*. Undergraduate Thesis. Universidad de los Andes, Bogotá, Colombia.

Recchi G. and Metti A., 1975. Lamina 17. In: Molo J.C. (Ed.), *Atlas Nacional de Panama*. Tommy Guardia, Panama City, Panama.

Silver E., Galewsky J. and McIntosh K., 1995. Variation in structure, style, and driving mechanism of adjoining segments of the North Panama deformed belt. *Geol. Soc. Am. Spec. Pap.*, **295**, 225–234.

Silver E.A., Reed D.L., Tagudin J.E. and Heil D.J., 1990. Implications of the north and south Panama thrust belts for the origin of the Panama orocline. *Tectonics*, **9**, 261–281.

Torsvik T.H., Müller R.D., Van der Voo R., Steinberger B. and Gaina C., 2008. Global plate motion frames: toward a unified model. *Rev. Geophys.*, **46**(3), RG3004, DOI: 10.1029 /2007RG000227.

Trela J., Vidito C., Gazel E., Herzberg C., Class C., Whalen W., Jicha B., Bizimis M. and Alvarado G.E., 2015. Recycled crust in the Galápagos Plume source at 70 Ma: Implications for plume evolution. *Earth Planet. Sci. Lett.*, **425**, 268–277.

Urdaneta M.P., 2016. *Geochemical and Petrological Characterization of Gabbroic Bodies in the Azuero Peninsula: Regional Implications*. Undergraduate Thesis. Universidad de los Andes, Bogotá, Colombia.

Vogt P.R., Lowrie A., Bracey D.R. and Hey R.N., 1976. Subduction of aseismic oceanic ridges: Effects on shape, seismicity, and other characteristics of consuming plate boundaries. *Geol. Soc. Am. Spec. Pap.*, **172**, 1–59.

Wegner W., Wörner G., Harmon R.S. and Jicha B.R., 2011. Magmatic history and evolution of the Central American Land Bridge in Panama since Cretaceous time. *Bull. Geol. Soc. Amer.*, **123**, 725–743.

Wallace L.M., McCaffrey R., Beavan J. and Ellis S., 2005. Rapid microplate rotations and backarc rifting at the transition between collision and subduction. *Geology*, **33**, 857–860, DOI: 10.1130/G21834.1

Whattam S.A, Montes C., McFadden R.R, Cardona A., Ramirez D. and Valencia V., 2012. Age and origin of earliest adakitic-like magmatism in Panama: Implications for the tectonic evolution of the Panamanian magmatic arc system. *Lithos*, **142**, 226–244.